NASW-4011

PRELIMINARY DEVELOPMENT OF A GLOBAL 3-D MAGNETOHYDRODYNAMIC COMPUTATIONAL MODEL FOR SOLAR WIND/COMETARY AND PLANETARY INTERACTIONS

(NASA-CR-177090) PRELIMINARY DEVELOPMENT OF A GLOBAL 3-D MAGNETOHYDRODYNAMIC COMPUTATIONAL MODEL FOR SOLAR WIND-COMETARY AND PLANETARY INTERACTIONS (Resource Management Associates, Inc.) 20 p CSCL 03B G3/92

N86-30621

Unclas 43549

RESOURCE MANAGEMENT ASSOCIATES

PRELIMINARY DEVELOPMENT OF A GLOBAL 3-D
MAGNETOHYDRODYNAMIC COMPUTATIONAL MODEL
FOR SOLAR WIND/COMETARY AND
PLANETARY INTERACTIONS

by

Stephen S. Stahara

RMA TR 101
May 1986

prepared under Contract No. NASW-4011

for

National Aeronautics and Space Administration
Washington, D.C. 20546

by

Resource Management Associates, Inc.
3738 Mt. Diablo Blvd., Suite 200
Lafayette, CA 94549
(415) 284-9071

TABLE OF CONTENTS

1. SUMMARY

This is the final summary report by Resource Management Associates, Inc., of the first year's work under Contract No. NASW-4011 to the National Aeronautics and Space Administration. The work under this initial phase of the contract relates to the preliminary development of a global, 3-D magnetohydrodynamic computational model to quantitatively describe the detailed continuum field and plasma interaction process of the solar wind with cometary and planetary bodies throughout the solar system. The work extends a highly-successful, observationally-verified computational model previously developed by the author, and is appropriate for the global determination of supersonic, super-Alfvenic solar wind flows past planetary obstacles. This report provides a concise description of the problems studied, a summary of all the important research results, and copies of the publications.

2. PROGRAM OVERVIEW

The overall objective of the present program relates to the development of a global, 3-D magnetohydrodynamic computational model to quantitatively describe the detailed continuum field and plasma interaction process of the solar wind with cometary and planetary bodies. The work involves detailed extensions of a highly-successful, observationally-verified solar wind/terrestrial planet interaction model previously developed by the principal investigator. That model, for reasons of computational efficiency, was preliminarily developed based upon a gas dynamic plus convected field approximation to the full MHD equations. In this program that model is being extended to the general 3-D MHD level and will additionally be generalized to include mass addition effects due to such phenomena as photoionization and charge exchange. The technical work of this study involes new computational development and numerical modeling of a variety of detailed and advanced aspects of the 3-D solar wind interaction problem. The ultimate goal is the development of a comprehensive, user-oriented, solar wind/cometary-planetary obstacle interaction computational model that would embody a hierarchy of three different accuracy levels and associated computational algorithms. For reasons that were described in detail in the original proposal, this hierachy of different accuracy levels is:

Level	Model
1	Axisymmetric gas dynamic + convected $\underset{\sim}{B}$ field
2	3-D gas dynamic + 3-D convected $\underset{\sim}{B}$ field
3	3-D MHD

A major objective of the first phase of the present study is to develop the Level 2 3-D gas dynamic plus 3-D convected $\underset{\sim}{B}$ field model. For reasons also described in detail in the original proposal, all 3 levels of the model will contain two separate flow field solvers that are coupled together to determine the steady state flow field. This feature of our model, which is unique among all currently existing global interaction models, allows very high resolution of the entire flow field, particularly in the tail region. This is illustrated in Figure 1, where a typical flow field grid density of the combined Level 1 axisymmetric flow solvers is shown. The region from the subsolar point to the terminator plane is solved via a time marching solver (NOSE code) to the steady state; whereas the region downstream of the terminator is solved via a spatially marching solver (TAIL code) which advances the solution downstream as far as required. As can be seen, the downstream grid density remains at very high resolution. Such detail of the downstream flow field cannot be achieved by any of the other currently existing interaction models which employ a single unsteady flow solver to determine the entire nose plus tail flow regions. The major technical tasks involved in the development of the Level 2 model are the development of the 3-D versions of the NOSE and

TAIL flow field codes (NOSE3D, TAIL3D). In addition, an entirely new magnetic field solver (MAG3D) to determine the convected $\underset{\sim}{B}$ field in a general 3-D gas dynamic flow field is also required. This requirement is necessary since the decomposition method of Alksne and Webster (Ref. 1) employed in the Level 1 axisymmetric model is valid only for axisymmetric flow fields and cannot be applied to general 3-D flows.

In addition to the development of the 3-D Level 2 model, several other technical tasks were planned for this first phase. These involve several extensions of the Level 1 model, and include preliminary development of a mass loading capability to account for such phenomena as photoionization and charge exchange, a complete diagnostic and analysis graphics package for detailed presentation of plasma and field properties throughout the magnetosheath, and a self-consistent procedure to determine the correct rather than approximate magnetoionopause shape and which locally satisfies the appropriate balance between magnetosheath and magnetospheric or ionospheric pressures across the magnetoionopause boundary. Finally, in addition to these model developments, a variety of collaborative investigations and applications involving the model were undertaken by us together with a number of space scientists. All of these developments are discussed in the following section.

3. PHASE I ACCOMPLISHMENTS

The major technical accomplishment of the Phase I effort involved the development of the sophisticated 3-D Level 2 gas dynamic flow field and convected $\underset{\sim}{B}$ field solvers. To accomplish this, it was necessary to develop and integrate three separate codes. Two of these codes are for determination of the flow field, and correspond to the 3-D versions of the NOSE and TAIL codes (NOSE3D, TAIL3D) shown in Figure 1. The third code (MAG3D) determines the convected B field in a general 3-D gas dynamic flow field. We provide a brief discussion of the development of these codes below.

After an extensive review of existing methods, selection of the basic solver to be employed in the NOSE3D code was made. The methodology is based upon the AIR3D code developed at NASA/Ames Research Center (Ref. 2). The solution algorithm employed is the Beam and Warming implicit approximate factorization algorithm used in delta form described in Ref. 3. The original basic algorithm is first-order accurate in time, noniterative, second-order accurate in spatial derivatives with central difference operators. This methodology is capable of solving both the inviscid gas dynamic Euler equations as well as, if required, a certain form of the viscous gas dynamic equations known as the thin-layer Navier-Stokes equations. These equations include certain additional terms over and above the Euler equation level which represent viscous effects in the body-normal direction. This capability is important to our study for future planned applications in which we wish to study certain viscous effects near the magnetoionopause boundary. The computational mesh employed in this method is one which incorporates a fitted shock outer boundary which exactly satisfies the unsteady, 3-D Rankine-Hugoniot relations and moves with the shock during the convergence process. The inner boundary is implemented as a fitted stationary surface representing the magnetoionopause surface. A mesh clustering capability for high density clustering in the body-normal direction has been implemented specifically to enable accuracy to be maintained for viscous calculations.

The gas dynamic solver employed for the Level 2 solution of the 3-D tail region of the flow field is based on the 3-D gas dynamic marching code reported in Ref. 4. The solution algorithm is a shock capturing, fully conservative form that employs second-order noncentered spatial derivatives to solve the steady, inviscid, gas dynamic Euler equations. As with the NOSE3D code, the mesh to be used with the TAIL3D code will employ a fitted outer boundary for the bow shock, at which location the steady 3-D Rankine-Hugoniot relations are exactly satisfied. The inner boundary of the mesh will also be fitted but to an impenetrable surface representing the magnetoionopause boundary.

The method chosen to determine the convected $\underset{\sim}{B}$ field for a general 3-D gas dynamic flow field involves the 3-D generalization of the kinematic procedure described by Spreiter in Ref. 5. In our implementation of the method, we have formulated a particularly efficient procedure. We initiate a streamline computation at the point in the magnetosheath where the $\underset{\sim}{B}$ field solution is desired. The streamline computation is then carried upstream through the bow shock into the uniform oncoming flow. At a selected point on that streamline in the uniform oncoming flow, a vector of incremental length centered about that point is formed in the direction of the oncoming IMF. Two streamlines that bracket the original streamline and which past through the ends of the incremental $\underset{\sim}{B}$ vector are then integrated downstream, at equal time steps with the original streamline, until they reach the original point in the magnetosheath where the $\underset{\sim}{B}$ field is desired. The direction and magnitude of the $\underset{\sim}{B}$ field are then given directly by the stretched and rotated incremental $\underset{\sim}{B}$ vector. This procedure is repeated at each point in the magnetosheath where the 3-D magnetic field is required.

Thus far in this phase, we have completed the initial development of all three of the above codes. The NOSE3D code, which requires by far the most computational resources since it integrates the unsteady 3-D Euler equations forward in time to a steady state, has now been developed and verified on a number of benchmark cases. We have similarly completed development and verification of the TAIL3D code. Finally, we have coupled the NOSE3D and TAIL3D codes via a joining data plane at the terminator location, and have initially verified the coupling procedure by performing several benchmark cases in which TAIL3D solutions were carried sufficiently far downstream from the terminator to demonstrate that a stable and accurate coupled solution procedure has been achieved. Similarly, we have developed the MAG3D code, and have initially verified it via comparisons with the Level 1 $\underset{\sim}{B}$ field procedure for the special case of axisymmetric flow.

In addition to the Level 2 3-D model development, we have developed in this phase a number of extensions and enhancements in the Level 1 model. These include a complete diagnostic and analysis graphics package that provides all of the detailed plasma and field properties throughout the interactive magnetosheath region. The package includes: maps of the plasma streamlines, velocity, temperature, and density contours; magnetic field contours and field line patterns; spacecraft trajectory diagrams in ecliptic and polar plane view; time histories of plasma density, temperature, velocity, magnitude and three velocity components; magnetic field magnitude and three magnetic field components; maps of entire computational grid; plots displaying the variation along arbitrary segments of the computational mesh of velocity magnitude and three velocity components, density, pressure, temperature, and magnetic field magnitude and three magnetic field components. The graphics package was intentionally based on CALCOMP routines for easy portability to other computer facilities. All of the plots included in the package have now been verified, and the package has been developed for use on a high-density dot matrix printer, a feature never before available with the model. The output from the graphics package is essentially report quality, and the capability provides for the first time the means for instantaneous viewing of the model results at almost no cost. Figures 2-4 provide some examples of an abbreviated subset of the complete grahical output of the analysis package, while Figures 5-7 provide corresponding examples of the diagnostic package.

With regard to the preliminary development of a mass loading capability in the Level 1 model, at this time we have completed derivation of the appropriate source model representation for mass loading due to photoionoization, and have also derived the appropriate modifications to the partial differential equations describing the conservation of mass, momentum, energy, and magnetic flux when such source terms due to this phenomena are present. Final development, individual implementation into both the NOSE and TAIL codes, and verification of the capability, together with case studies at Venus, will be completed in Phase II.

We have also proceeded to develop a self-consistent iterative procedure in the Level 1 model to improve the satisfaction of the pressure balance boundary condition at the magnetoionopause boundary. The present Level 1 model employs a specified magnetoionopause shape that is previously determined using a Newtonian surface pressure variation from the stagnation point to points along the surface up to the terminator. This variation is used to approximate the pressure distribution on the magnetosheath side of the magnetoionopause. The improved procedure we are developing will iteratively alter that initial shape so as to ultimately satisfy the true pressure balance that locally exists between the exact magnetosheath plasma and magnetospheric/ionospheric pressure at each point along the magnetoionopause boundary.

4. COLLABORATIVE INVESTIGATIONS

Finally, in addition to all of the model developments described above, we have also carried out a variety of collaborative investigations involving use of the model. These studies were undertaken by us together with a number of space scientists. We consider these investigatons to be one of the most important aspects of the model development being undertaken here, as they effectively guarantee the widespread utility of the model through interdisciplinary studies involving many different topics of current space science interest.

A list of the publications that have resulted from those particular studies and which are now complete is as follows:

Publications from Completed Collaborative Studies

Magnetopause Merging Site Asymmetries, N. U. Crooker, J. G. Luhmann, J. R. Spreiter and S. S. Stahara. Jour. Geophys. Res., Vol. 90, No. A1, January 1985, pp. 341-346.

Magnetic Field Draping Against the Dayside Magnetopause, N. U. Crooker, J. G. Luhmann, C. T. Russell, E. J. Smith, J. R. Spreiter and S. S. Stahara. Jour. Geophys. Res., Vol. 90, No. A4, April 1985, pp. 3505-3510.

Solar Wind Flow About the Outer Planets: Gasdynamic Modeling of the Jupiter and Saturn Bow Shocks, J. A. Slavin, E. J. Smith, J. R. Spreiter and S. S. Stahara. Jour. Geophys. Res., Vol. 90, No. A7, July 1985, pp. 6275-6286.

Evidence for Mass-Loading of the Venus Magnetosheath, J. G. Luhmann, C. T. Russell, J. R. Spreiter and S. S. Stahara. Adv. Space Res., Vol. 5, No. 4, 1985, pp. 307-311.

A Gas Dynamic Magnetosheath Field Model for Unsteady Interplanetary Fields: Application to the Solar Wind Interaction with Venus, J. G. Luhmann, R. J. Warniers, C. T. Russell, J. R. Spreiter and S. S. Stahara. Jour. Geophys. Res., Vol. 91, No. A3, March 1985, pp. 3001-3010.

Magnetohydrodynamic and Gasdynamic Theories for Planetary Bow Waves, J. R. Spreiter and S. S. Stahara. Geophysical Monograph 35, <u>Collisionless Shock Waves in the Heliosphere: Reviews of Current Research</u>, 1985. 1985.

In addition to these completed studies, we are also currently engaged in other collaborative studies involving use of the model. These include: (1) studies involving the quantitative determination of 3-D effects of the solar wind interaction with the asymmetric magnetopauses of Jupiter and Saturn - with Dr. James Slavin and

Dr. Edward Smith of JPL; (2) studies of the predicted and observed ionopause shapes at Venus when the exact local plasma pressure in the magnetosheath is balanced with the observed local ionospheric pressure - with Dr. William Knudsen of Knudsen Geophysical Research.

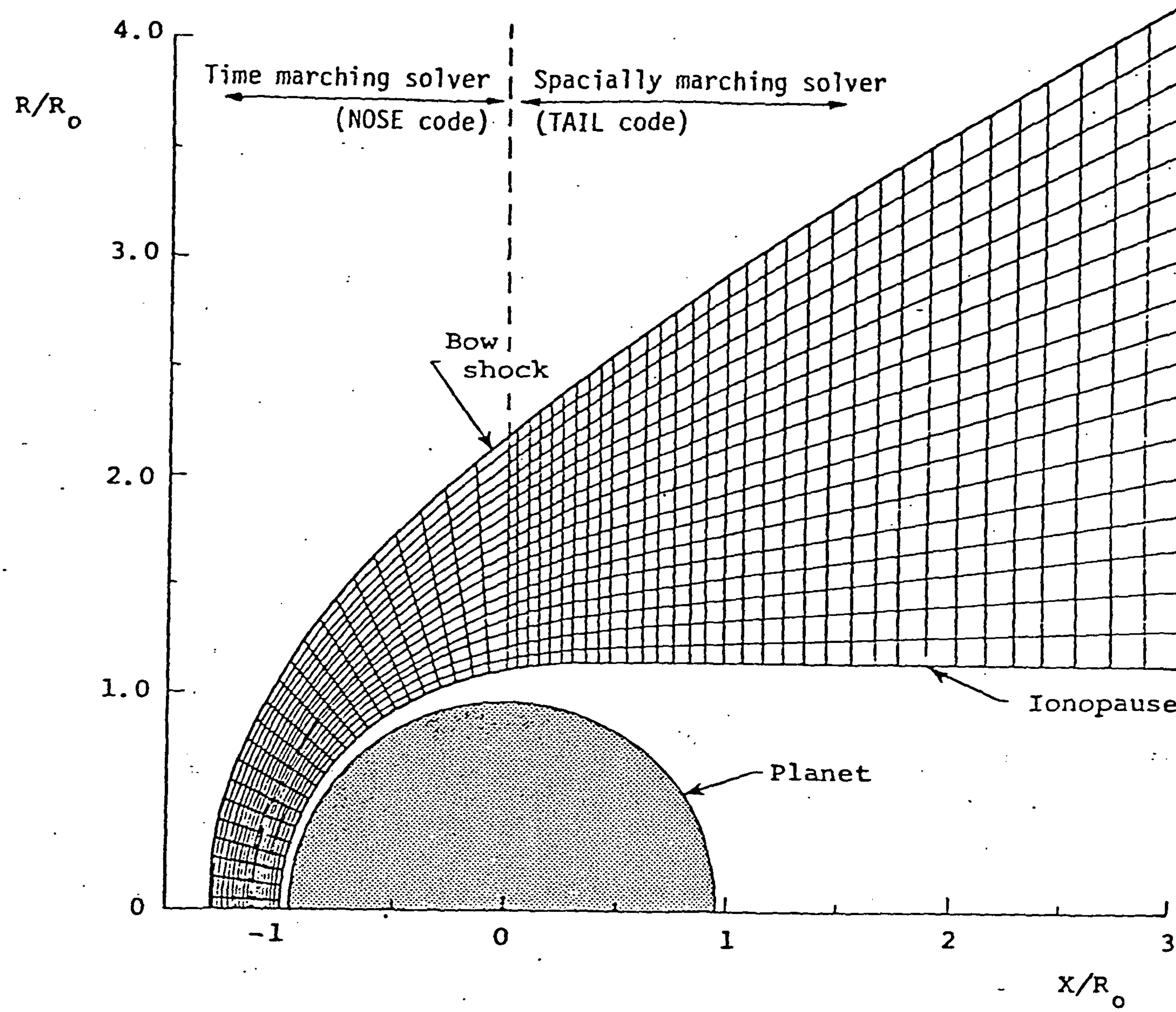

Figure 1. Illustration of typical flow-field grid density for Level 1 model; $M_\infty = 3.0$, $\gamma = 5/3$, $H/R_0 = 0.03$

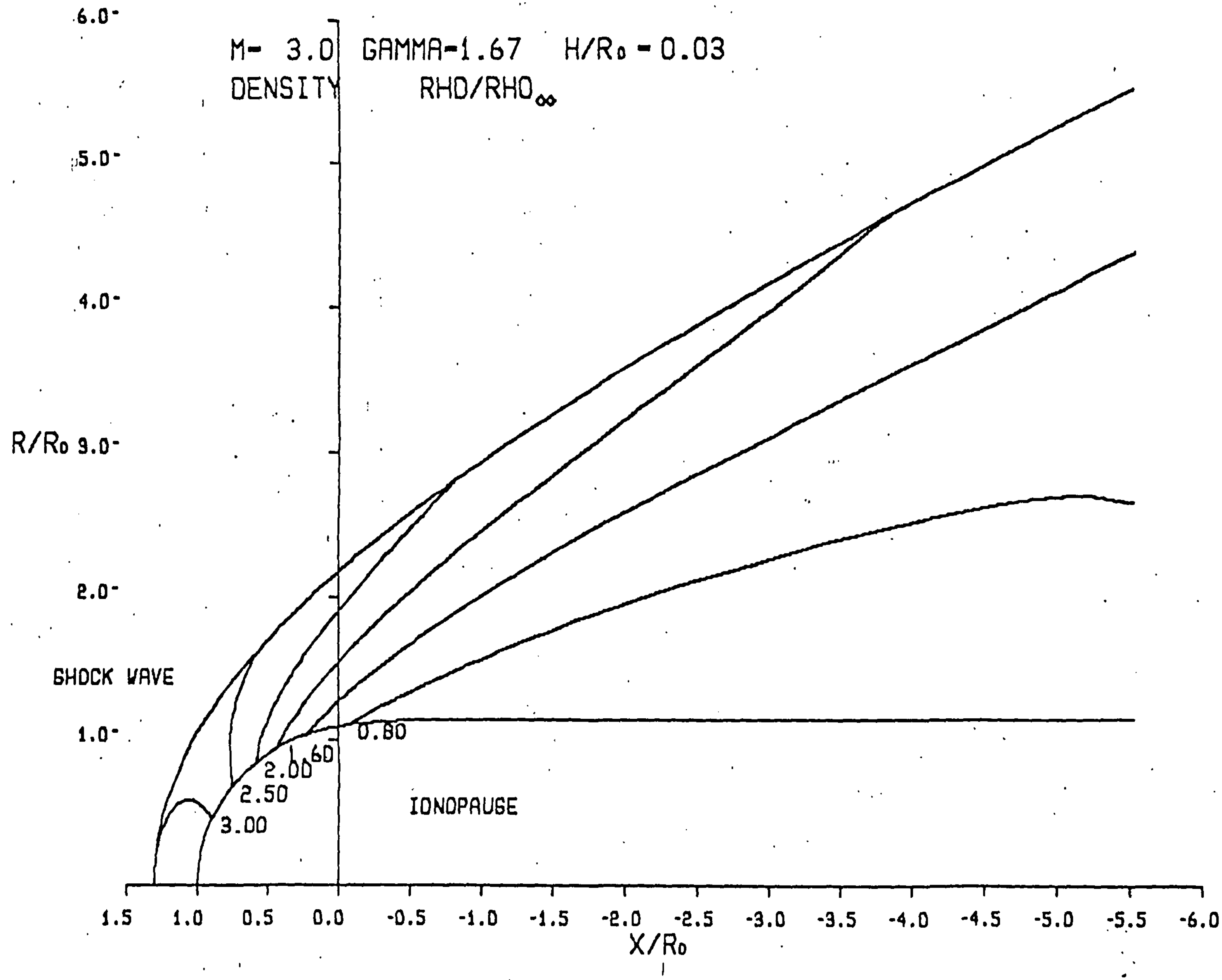

Figure 2. Sample flow field output from Level 1 model graphical output package: density contours for $M_\infty = 3.0$, $\gamma = 5/3$ flow past an ionopause shape with $H/R_0 = 0.03$

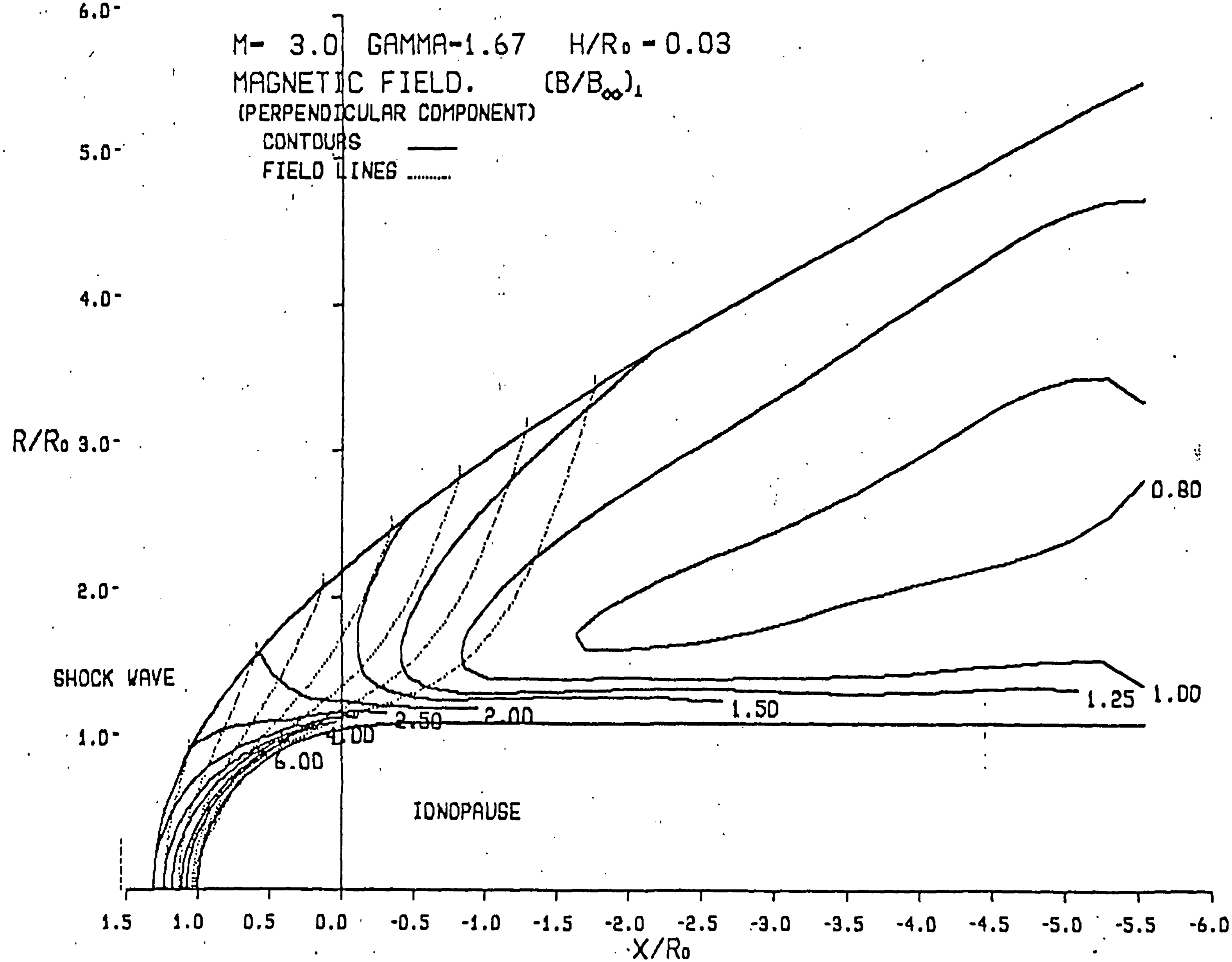

Figure 3. Sample magnetic field output from Level 1 model graphical output package: magnetic field lines and contours for perpendicular field component for $M_\infty = 3.0$, $\gamma = 5/3$, $H/R_0 = 0.03$ ionopause obstacle flow

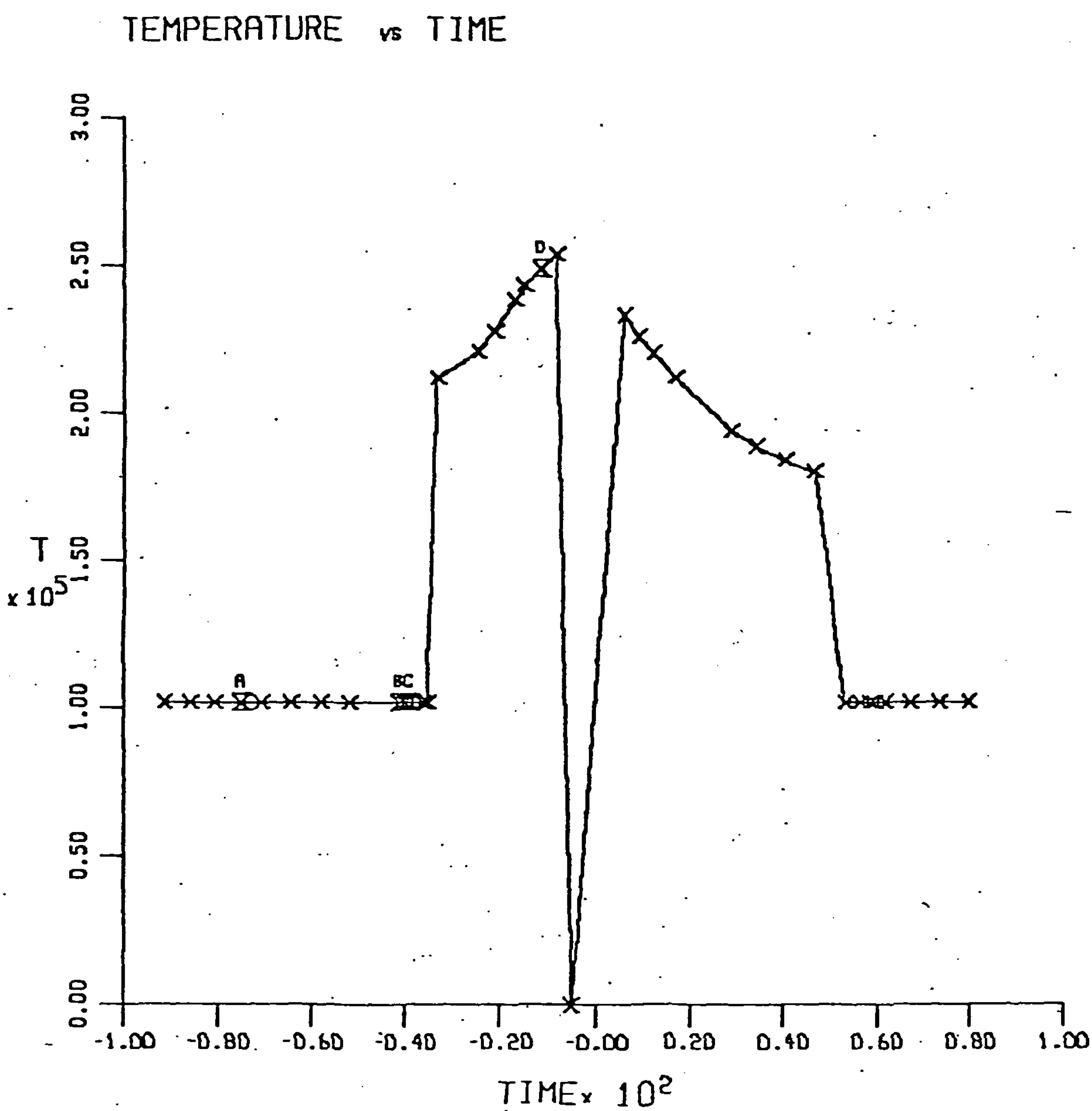

Figure 4. Sample time history output from Level 1 model graphical output package: temperature vs. time for a trajectory passing through the magnetosheath region and ionopause of the flow field shown in Figure 1

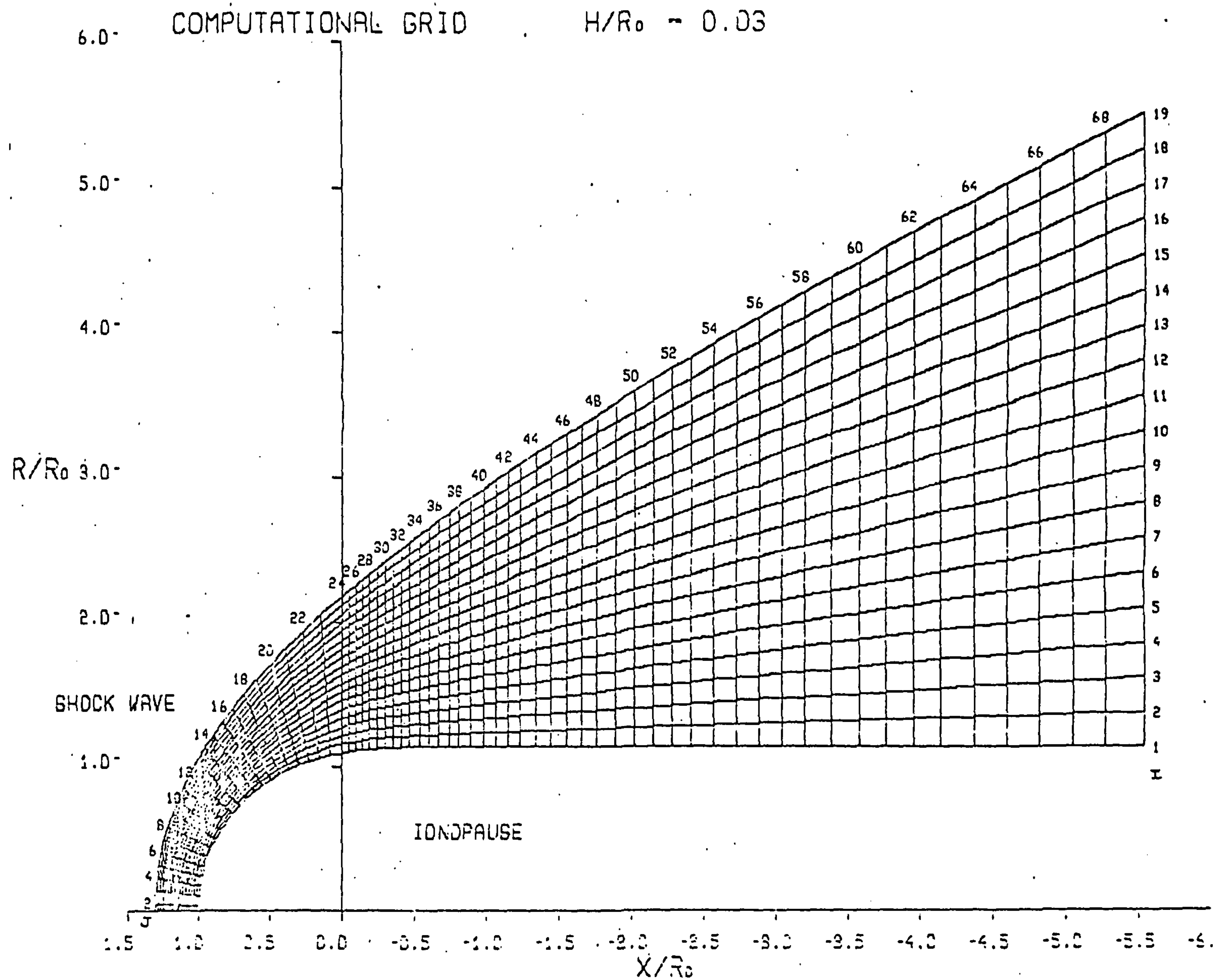

Figure 5. Sample plot from Level 1 model extended diagnostic graphic output package: computational grid for $M_\infty = 3.0$, $\gamma = 5/3$ flow past an ionopause shape with $H/R_0 = 0.03$

ORIGINAL PAGE IS OF POOR QUALITY

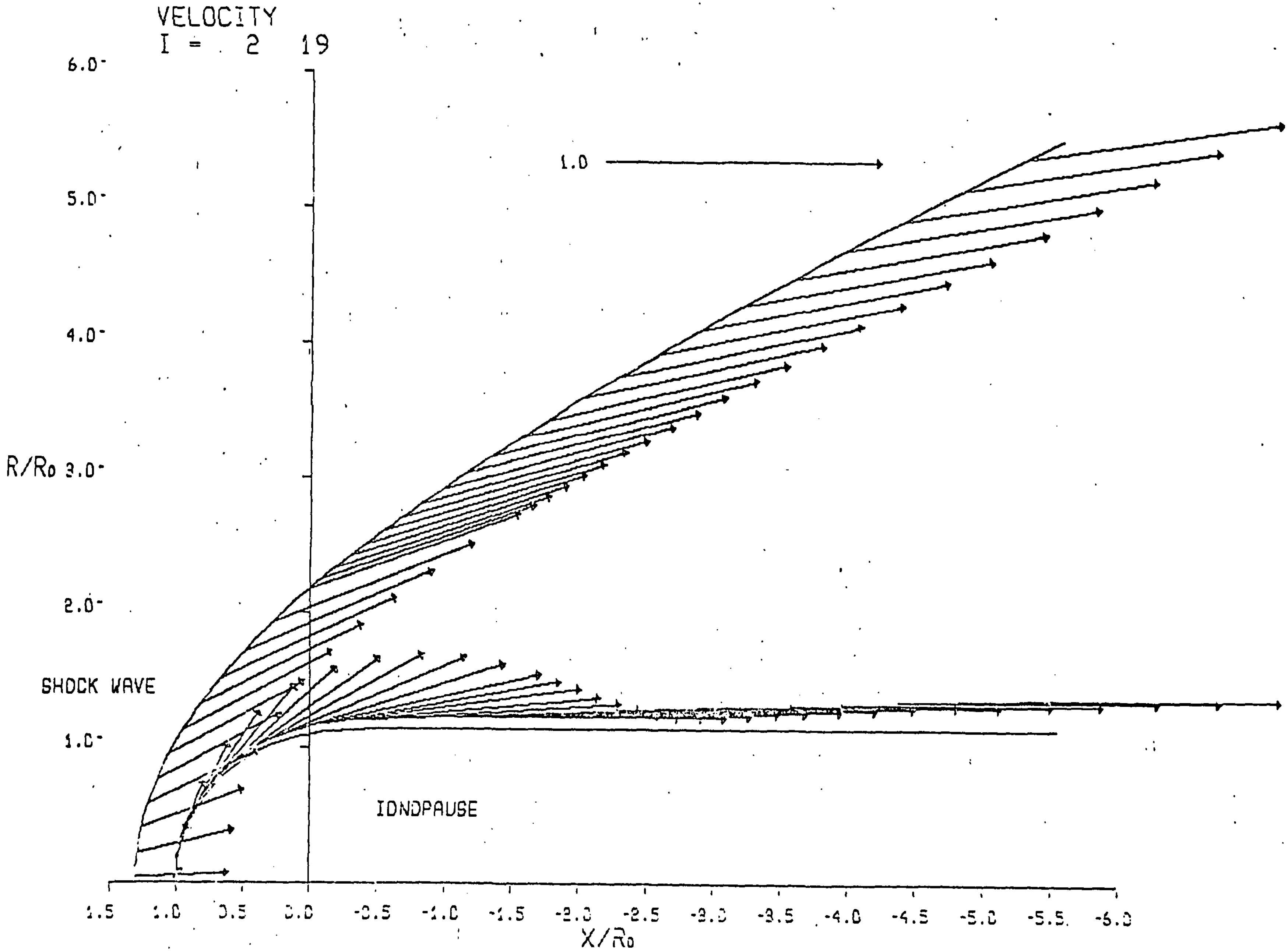

Figure 6. Sample plasma property output from Level 1 model extended diagnostic graphic output package: velocity vector plots along constant radial mech locations at one mesh spacing away from the obstacle surface (I=2) and along bow shock (I=19)

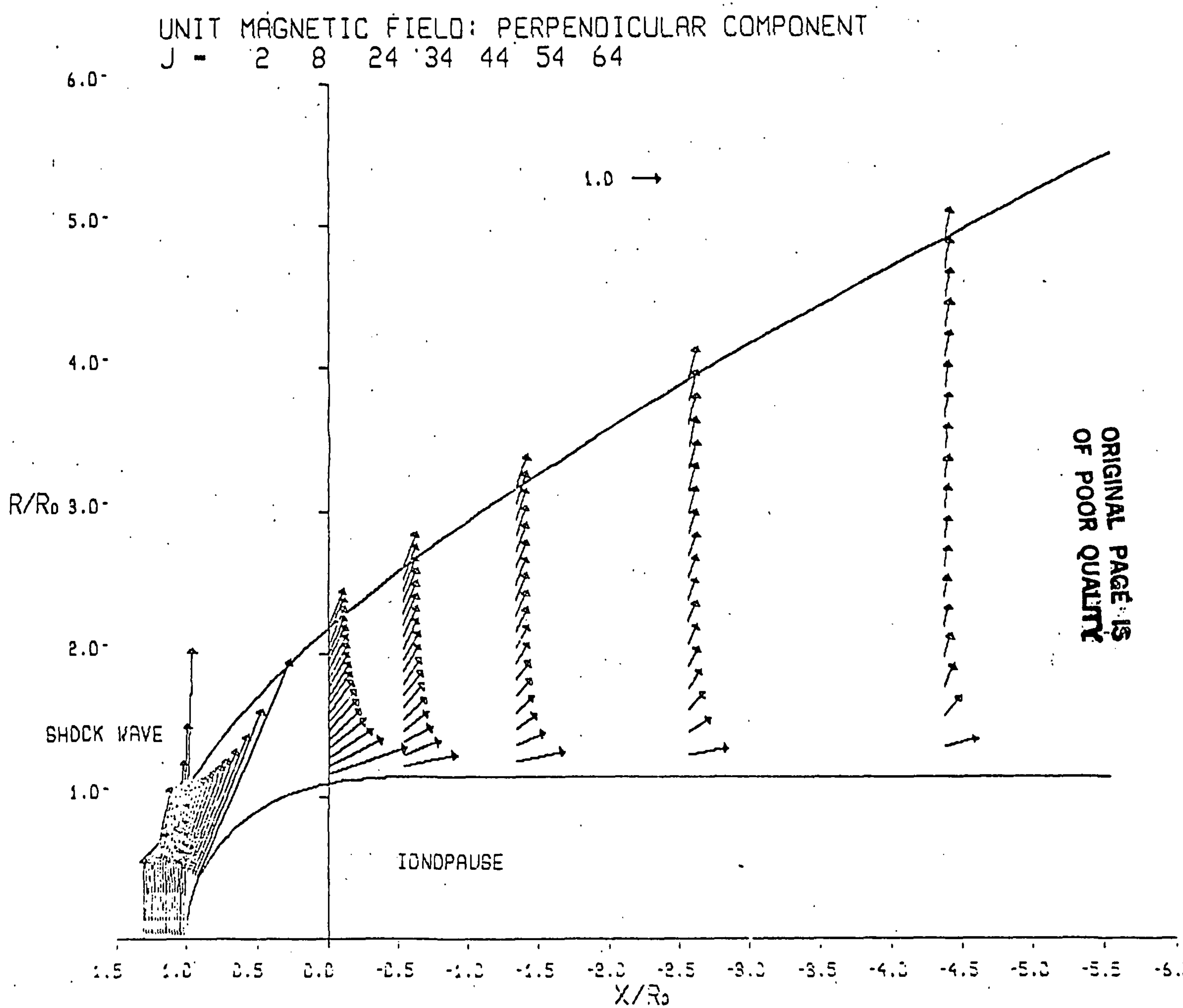

ORIGINAL PAGE IS OF POOR QUALITY

Figure 7. Sample magnetic field output from Level 1 model extended diagnostic graphic output package: vector plots of unit magnetic field perpendicular component along various radial mesh lines normal to the obstacle for $M_\infty = 3.0$, $\gamma = 5/3$ flow past an ionopause shape with $H/R_0 = 0.03$

REFERENCES

1. Alksne, A. Y. and Webster, D. L.: Magnetic and Electric Fields in the Magnetosheath. Plan. and Space Sci., Vol. 18, pp. 1203-1212, 1970.

2. Pulliam, T. H. and Steger, J. L.: On Implicit Finite-Difference Simulations of Three-Dimensional Flow. AIAA Paper 78-10, January 1978.

3. Beam, R. and Warming, R. F.: An Implicit Factored Scheme for the Compressible Navier-Stokes Equations. AIAA Paper 77-645, June 1977.

4. Kutler, P., Warming, R. F. and Lomax, H.: Computation of Space Shuttle Flow Fields Using Noncentered Finite-Difference Schemes. AIAA Journal, Vol. 11, No. 2, February 1973, pp. 196-204.

5. Spreiter, J. R. and Alksne, A. Y.: Solar Wind Flow Past Objects in the Solar System. Annual Rev. of Fluid Mechanics, Vol. 2, pp. 313-354, Ed. M. D. Van Dyke and W. G. Vincenti, 1970.

APPENDIX

TABLE OF CONTENTS